High-efficiency continuously tunable single-frequency doubly resonant optical parametric oscillator

Chunchun Liu, Xiaomin Guo, Zengliang Bai, Xuyang Wang, and Yongmin Li*

State Key Laboratory of Quantum Optics and Quantum Optics Devices, Institute of Opto-Electronics,
Shanxi University, Taiyuan 030006, China

*Corresponding author: yongmin@sxu.edu.cn

We report a high-efficiency continuously tunable single-frequency doubly resonant optical parametric oscillator (OPO) based on periodically poled KTiOPO4. Pumped by a frequency-doubled Nd:YLF laser at 526.5 nm, the OPO has a low threshold of 30 mW and can deliver up to 156 mW single-frequency output at $0.8\,\mu m$ and 89 mW single-frequency output at $1.5\,\mu m$ with 390 mW of pump power. Coarse and continuous frequency tuning are also demonstrated experimentally.   © 2011 Optical Society of America

OCIS codes: 190.4970, 140.3480.

1. Introduction

Continuous wave optical parametric oscillators (OPO) are attractive sources of wide tunable and narrow linewidth single-frequency radiation in spectral regions inaccessible to lasers. At present, cw singly resonant OPO (SROPO) can generate several watts of single-frequency output thanks to the availability of high-quality single-frequency solid-state lasers and various quasi-phase-matched (QPM) materials. Because of their high output power and robust stability, SROPOs are getting a lot of attentions. However, it is known that high pump power (the order of 10 W) is usually required to operate such devices. In some applications, tunable single-frequency radiation with power of 100 mW is enough. In this case, a tunable doubly resonant OPO (DROPO) is a better choice for its low-pump threshold.

The first cw DROPO was demonstrated by Smith *et al.* [1]; almost at the same time, Byer *et al.* also reported a cw DROPO system [2]. Both of these pioneering experiments utilized multimode lasers as the pump source, and the OPO cavity length was not actively stabilized. It seemed that the DROPOs were highly unstable and difficult to tune, and then they were forgotten for a long time. Later, cw DROPOs regained attention due to the significant improvements in single-frequency laser, new cavity designs, novel nonlinear materials, and progress of cavity locking. Nabors *et al.* reported a single-frequency operation of a monolithic OPO with a threshold of 12 mW and total output power of 8.15 mW [3]. Breitenbach *et al.* obtained an 81% conversion efficiency with a monolithic OPO; the threshold is 28 and 105 mW combined signal, and idler output power was achieved at a pump power four times above threshold [4]. Bode *et al.* reported a nearly 400 mW total output power with a conversion efficiency of less than 40% based on a semimonolithic OPO [5]. By using active stabilization, the work of Al-Tahtamouni *et al.* showed that the DROPO could operate on a single-mode pair for 18 h without mode hops [6]. Besides the demonstrations of stable and efficient single-frequency operation of cw DROPOs, broad continuous frequency tuning was also achieved experimentally. Henderson *et al.* demonstrated continuous signal tuning of 17 GHz and idler tuning of 10 GHz by simultaneously controlling the cavity length of the OPO and the frequency of the pump laser [7].

The purpose of this work is to extend previous investigations to achieve an efficient and continuously tunable DROPO that can generate

single-frequency coherence radiation around 0.8 and 1.5 μm. Although several works have reported the generation of single-frequency light at such wavelength range by using a DROPO, the conversion efficiency of their OPOs are very limited (less than 11%) [8–10]. It is known that the output power for a DROPO can be given by (Eq. (12) of [4] and Eq. (39) of [11])

$$P_j^{\text{out}} = 4P_{\text{th}} \frac{\omega_j}{\omega_p} \frac{T_j}{T_j + A_j} \left(\sqrt{\frac{P_{\text{in}}}{P_{\text{th}}}} - 1 \right), \quad (1)$$

where $j = s/i$ stands for the signal/idler. P_{th} is the pump threshold, P_{in} is the input mode-matching pump power, T_j is the transmission of the output coupler, and A_j is the residual intracavity round-trip linear loss. ω_j is the angular frequency of the signal/idler beam, and ω_p is the angular frequency of the pump beam. From Eq. (1), it is evident that the highest conversion efficiency, $\eta_{\text{max}} = P_j^{\text{out}}/P_{in} = (\omega_j/\omega_p)(T_j/(T_j + A_j))$, is reached at four times above threshold, $P_{\text{in}} = 4P_{\text{th}}$. In other words, a lower threshold is not necessarily good for high output power. For a given pump power P_{in}, the pump threshold has to be adjusted to be $P_{\text{th}} = P_{\text{in}}/4$ in order to maximize η_{max}. In an ideal situation where there is no residual intracavity linear loss, one can achieve a perfect conversion efficiency of 100%. In a realistic situation, the conversion efficiency is limited mainly by the escape efficiency of the OPO cavity $\eta_{\text{escape}} = T_j/(T_j + A_j)$. To improve the conversion efficiency, one needs a high η_{escape}; that means A_j should be much smaller than T_j. A monolithic or a semimonolithic OPO is a good candidate for its high escape efficiency and superior cavity stability. However, this cavity design requires accurate polishing of the end faces and lacks flexibility in the changing of mirror coupling coefficients. For a discrete-element linear cavity (two mirrors and one crystal), a high η_{escape} can also be obtained by considering the following two points. First, the residual reflection losses and absorption at multiple surfaces can be minimized with high-quality optical coating of cavity mirrors and nonlinear crystal. Second, one can increase reasonably the transmission of the output coupler.

In this paper, we report a 526.5 nm pumped high-efficiency continuously tunable single-frequency discrete-element DROPO based on periodically poled KTiOPO4 (PPKTP). To improve the conversion efficiency, an output mirror with a relatively high transmission ratio was adopted to ensure a high escape efficiency. The OPO has a threshold of 30 mW and can deliver 245 mW single-frequency output at 0.8 and 1.5 μm with the corresponding conversion efficiency of 63%. Coarse and continuous frequency tuning characteristics are also investigated experimentally.

2. Experimental Setup and Results

Figure 1 is the schematic diagram of the DROPO system. The pump source is a 526.5 nm Nd:YLF/KTP intracavity frequency-doubling single-frequency laser providing an output power of 500 mW. The laser can be continuously tuned over a range of ~7.4 GHz by scanning the cavity length using a piezoelectric transducer (PZT) [12]. A Faraday isolator was set in the input light of the DROPO to eliminate the backreflection. The OPO cavity was mounted on an Invar base plate and contained in a box. It consists of two planoconcave mirrors with 30 mm radii of curvature, and the beam waist of the resonator is about 50 μm inside the nonlinear crystal. The input coupler was coated for high reflectivity at 0.8 and 1.5 μm ($R > 99.8\%$) and high transmission at 526.5 nm ($T > 96\%$). The output coupler was coated for high reflectivity at 526.5 nm ($R > 99.8\%$) and partial transmission ($T \sim 5.5\%$) at 0.8 and 1.5 μm. A 20-mm-long PPKTP with a poling period of 9.68 μm was used as the nonlinear crystal for its relatively high nonlinear coefficient and room temperature operation. Both end faces of the PPKTP crystal were antireflection coated at 526.5 nm, 0.8, and 1.5 μm. The crystal was put in a temperature-controlled oven with stability of 0.005 °C.

A dither-locking method was used to stabilize the cavity length of the OPO to the peak of a signal-idler double resonance. In this way the OPO maintains amplitude-stable operation on a single signal-idler mode pair, and no mode hops were observed for as long as 60 min. A scanning confocal Fabry–Perot interferometer was used to monitor and verify single-frequency output of the DROPO; a typical interferometer spectral scan was shown in Fig. 2. The higher peaks are 1.5 μm idler, and the lower peaks are 0.8 μm signal. The difference between their intensities is due to the wavelength-dependent sensitivity of the detector and the coating characteristics of the interferometer. Behind the OPO cavity, a dichroic beam splitter was used to separate the signal beam and idler beam. Figure 3 shows the measured signal and idler power at signal wavelength of 805 nm as a function of incident pump power. The pump threshold of the OPO is 30 mW. Up to 156 mW single-frequency output at 805 nm
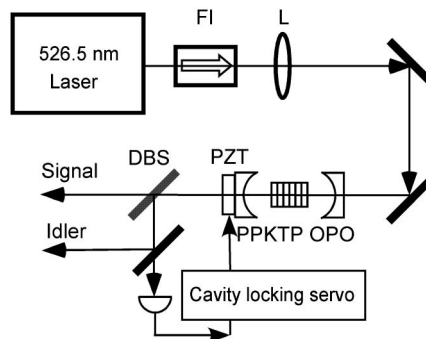

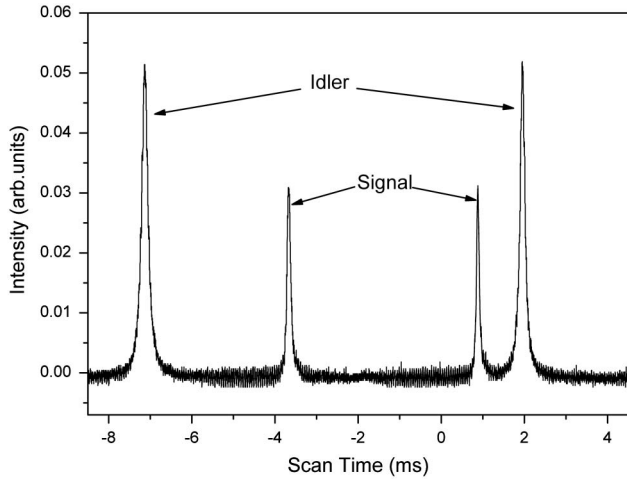Fig. 1. Schematic diagram of the DROPO system. FI, faraday isolator; L, lens; DBS, dichroic beam splitter.

Fig. 2. Single-frequency operation of the DROPO measured by a scanning confocal Fabry–Perot interferometer. The free spectral range (FSR) of the confocal Fabry–Perot interferometer is 375 MHz (FSR = $c/4L_{cav}$ = 375 MHz, L_{cav} is the cavity length). To span one FSR, the cavity length should be scanned by an amount of $\lambda/4$ (λ is the wavelength of the input light). In our case, the signal wavelength (0.8 μm) is about half of the idler wavelength (1.5 μm), this makes the different cavity-length interval for the FSR of the signal/idler.

and 89 mW single-frequency output at 1522 nm could be obtained with pump power of 390 mW, and the total down-conversion efficiency is 63%. The solid and dashed curves are the best theoretical fittings to experimental data by using Eq. (1) with the fitted value of T_j = 5.5% and A_j = 1.8%. It was found that when the pump power is higher than 390 mW, the OPO cannot maintain oscillation on a single signal-idler mode pair, and the OPO becomes the multimode output. A similar phenomenon was also observed in [13,14], and it was explained that several cluster curves can simultaneously oscillate when the pump power is much higher than the threshold of the DROPO.
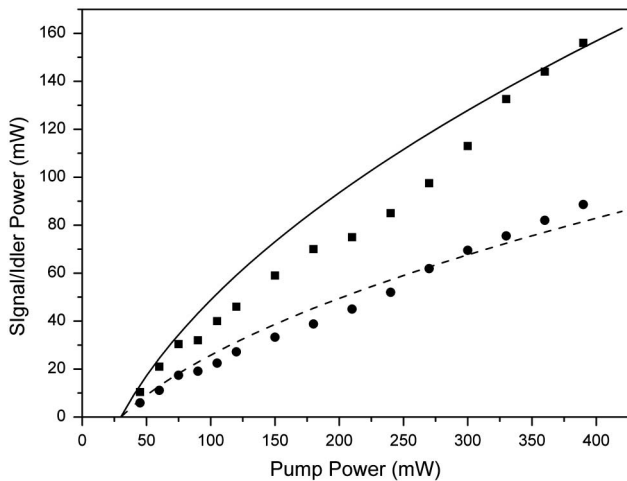

Fig. 3. The measured output power of the signal (solid squares) and idler (solid circles) beams versus the pump power. The solid and dashed lines are theoretical fittings for the signal and idler beams, respectively.

Coarse tuning of the signal and idler wavelengths can be conveniently achieved by varying the temperature of the PPKTP crystal. Figure 4 shows the temperature-tuning characteristics of the DROPO. For temperatures between 10 °C and 90 °C, the signal wavelength was measured with a high-precision wavemeter while scanning the OPO cavity length using the PZT. Signal wavelength from 791.29 to 807.53 nm was achieved. The corresponding idler wavelength tuning is from 1573.37 to 1512.87 nm. The theoretical tuning curves can be calculated using the Sellmeier equations of KTP and QPM conditions [15],

$$\Delta k_Q = k_p - k_s - k_i - \frac{2\pi}{\Lambda} = 0, \qquad (2)$$

where Λ is the poling period of PPKTP, and k_p, k_s, and k_i are wave vectors for the pump, signal, and idler, respectively. The OPO wavelengths can also be mode-hop tuned by scanning the OPO cavity length at a fixed temperature [15]. The measured signal tuning range is around 0.2 nm (the inferred value for the idler is 0.71 nm according to energy conservation relation $\omega_p = \omega_s + \omega_i$) when the cavity length is varied by half of the pump wavelength, then a cluster jump will occur (see inset of Fig. 4).

Continuous frequency tuning is required in many applications such as high-resolution spectroscopy. It is difficult to continuously tune the wavelength by adjusting only the parameters of the DROPO (such as the cavity length, crystal temperature, etc.). However, it was demonstrated that the output wavelengths of the DROPO can be tuned continuously by the continuous tuning of the pump laser frequency [7]. For a fixed crystal temperature and cavity length stabilized DROPO, the signal/idler tuning range versus the pump tuning can be approximated given as (by neglecting the dispersion of the nonlinear crystal) [6]

$$\delta\omega_j \approx \frac{\omega_j}{\omega_p}\delta\omega_p, \qquad (3)$$

where $j = s/i$. Figure 5 shows the continuous tuning results of the OPO. The cavity length servo kept the OPO locked to the same signal and idler mode pair as the pump frequency was changed continuously. The smooth tuning of the pump laser was followed by the smooth tuning of the OPO. The measured continuous frequency tuning range of the signal is 4.3 GHz, and this corresponds to idler tuning of 2.3 GHz. The continuous tuning range of the OPO is limited by the continuous tuning range of the pump laser.

3. Discussion and Conclusion

In summary, a high-efficiency continuously tunable single-frequency DROPO based on a PPKTP was demonstrated. Pumped by a frequency-doubled Nd:YLF laser at 526.5 nm, the OPO has a low threshold of 30 mW and can deliver up to 156 mW single-frequency output at 0.8 μm and 89 mW
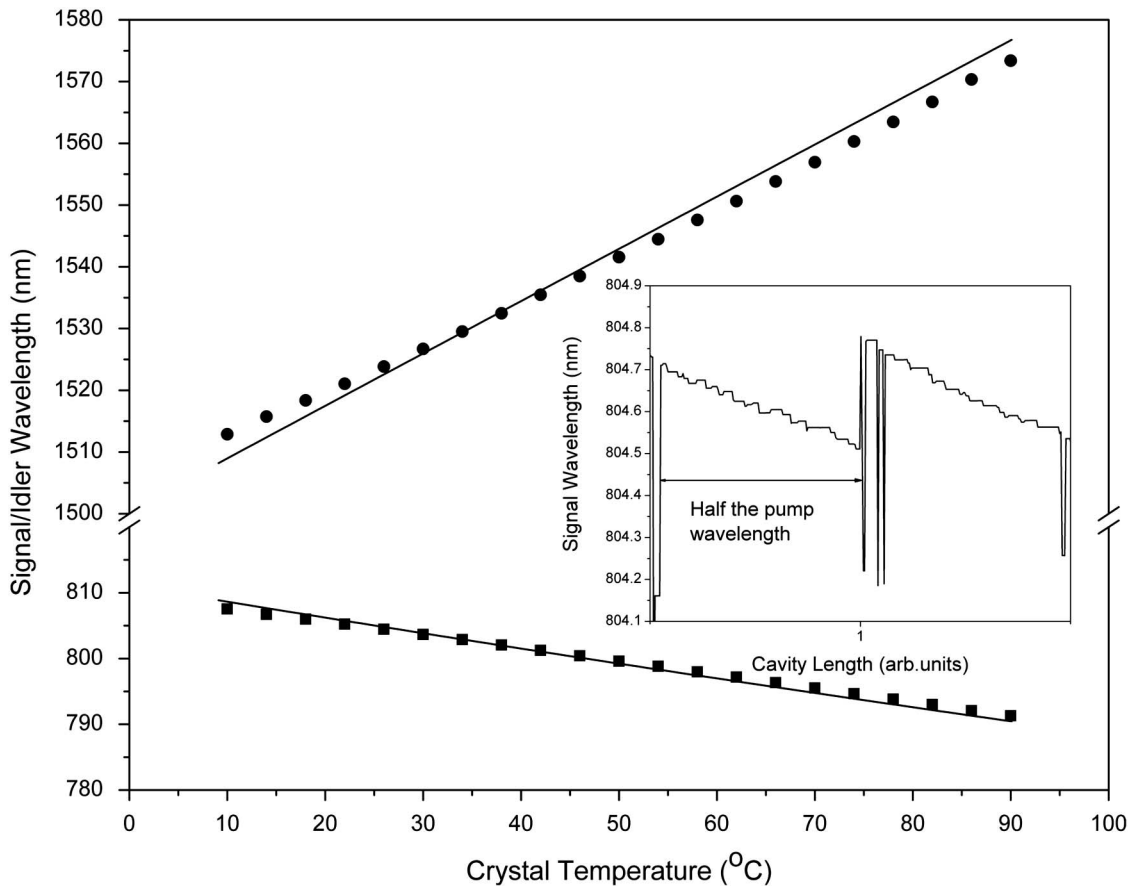
Fig. 4. OPO output wavelengths versus the crystal temperature. Solid square, signal; solid circles, idler. The solid lines are theoretical fittings calculated using QPM condition and the Sellmeier equations. Inset, mode-hop tuning by scanning the cavity length.

single-frequency output at $1.5\,\mu m$. By adjusting the crystal temperature and cavity length, the OPO wavelengths can be coarsely tuned over several tens of nanometers. Continuous frequency tuning of $4.3\,GHz$ for signal was also achieved by smooth tuning of the pump laser. The DROPO device presented here has potential applications in high-precision atomic and molecular spectroscopy [10,16]. For

example, the absorption lines of alkaline atoms (Rb, Cs) are around $0.8\,\mu m$ and the absorption spectra of acetylene are around $1.5\,\mu m$.
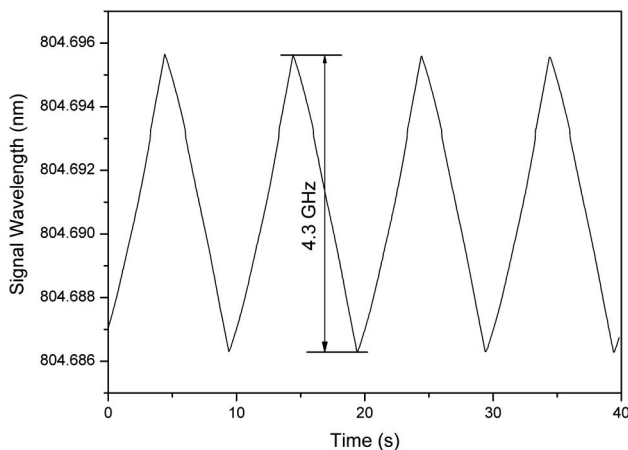
Fig. 5. OPO output wavelengths can be smoothly tuned by smooth tuning of the pump laser. The signal tuning range is $4.3\,GHz$, and the corresponding idler tuning is $2.3\,GHz$.

References

1. R. G. Smith, J. E. Geusic, H. J. Levinstein, J. J. Rubin, S. Singh, and L. G. Van Uitert, "Continuous optical parametric oscillation in $Ba_2NaNb_5O_{15}$," Appl. Phys. Lett. **12**, 308–310 (1968).
2. R. L. Byer, M. K. Oshman, J. F. Young, and S. E. Harris, "Visible cw parametric oscillator," Appl. Phys. Lett. **13**, 109–111 (1968).
3. C. D. Nabors, R. C. Eckardt, W. J. Kozlovsky, and R. L. Byer, "Efficient, single-axial-mode operation of a monolithic MgO:LiNbO$_3$ optical parametric oscillator," Opt. Lett. **14**, 1134–1136 (1989).
4. G. Breitenbach, S. Schiller, and J. Mlynek, "81% conversion efficiency in frequency-stable continuous-wave parametric oscillation," J. Opt. Soc. Am. B **12**, 2095–2101 (1995).
5. M. Bode, P. K. Lam, I. Freitag, A. Tünnermann, H.-A. Bachor, and H. Welling, "Continuously-tunable doubly resonant optical parametric oscillator," Opt. Commun. **148**, 117–121 (1998).

6. R. Al-Tahtamouni, K. Bencheikh, R. Storz, K. Schneider, M. Lang, J. Mlynek, and S. Schiller, "Long-term stable operation and absolute frequency stabilization of a doubly resonant parametric oscillator," Appl. Phys. B **66**, 733–739 (1998).

7. A. J. Henderson, P. M. Roper, L. A. Borschowa, and R. D. Mead, "Stable, continuously tunable operation of a diode-pumped doubly resonant optical parametric oscillator," Opt. Lett. **25**, 1264–1266 (2000).

8. M. Tsunekane, S. Kimura, M. Kimura, N. Taguchi, and H. Inaba, "Continuous-wave, broadband tuning from 788 to 1640 nm by a doubly resonant, MgO:LiNbO$_3$ optical parametric oscillator," Appl. Phys. Lett. **72**, 3414–3416 (1998).

9. T. Ikegami, S. Slyusarev, and S. I. Ohshima, "Long-term, mode-hop-free operation of a continuous-wave doubly resonant, monolithic optical parametric oscillator," Opt. Commun. **184**, 13–17 (2000).

10. T. Ikegami and H. Inaba, "Atomic and molecular spectroscopy with a continuous-wave, doubly resonant, monolithic optical parametric oscillator," Opt. Commun. **269**, 188–193 (2007).

11. E. Rosencher and C. Fabre, "Oscillation characteristics of continuous-wave optical parametric oscillators: Beyond the mean-field approximation," J. Opt. Soc. Am. B **19**, 1107–1116 (2002).

12. K. I. Martin, W. A. Clarkson, and D. C. Hanna, "Self-suppression of axial mode hopping by intracavity second-harmonic generation," Opt. Lett. **22**, 375–377 (1997).

13. R. C. Eckardt, C. D. Nabors, W. J. Kozlovsky, and R. L. Byer, "Optical parametric oscillator frequency tuning and control," J. Opt. Soc. Am. B **8**, 646–667 (1991).

14. A. J. Henderson, M. J. Padgett, F. G. Colville, J. Zhang, and M. H. Dunn, "Doubly-resonant optical parametric oscillators: tuning behavior and stability requirements," Opt. Commun. **119**, 256–264 (1995).

15. L. E. Myers, R. C. Eckardt, M. M. Fejer, R. L. Byer, W. R. Bosenberg, and J. W. Pierce, "Quasi-phase-matched optical parametric oscillators in bulk periodically poled LiNbO$_3$," J. Opt. Soc. Am. B **12**, 2102–2116 (1995).

16. J. Cousin, P. Masselin, W. Chen, D. Boucher, S. Kassi, D. Romanini, and P. Szriftgiser, "Application of a continuous-wave tunable erbium-doped fiber laser to molecular spectroscopy in the near infrared," Appl. Phys. B **83**, 261–266 (2006).